

Central Powering of the Largest Lyman-alpha Nebula is Revealed by Polarized Radiation

Matthew Hayes^{1,2,3}, Claudia Scarlata^{4,5}, and Brian Siana⁶

¹*Université de Toulouse, UPS-OMP; IRAP; Toulouse, France*

²*CNRS; IRAP; 14, avenue Edouard Belin, F-31400 Toulouse, France*

³*Observatory of Geneva, University of Geneva, 51 ch. des Maillettes, 1290 Versoix, Switzerland*

⁴*Minnesota Institute for Astrophysics, School of Physics and Astronomy, University of Minnesota, Minneapolis, MN 55455, USA*

⁵*Spitzer Science Center, California Institute of Technology, 220-6, Pasadena, CA 91125, USA*

⁶*Department of Astronomy, California Institute of Technology, MS 249-17, Pasadena, CA 91125, USA*

High-redshift Lyman-alpha blobs^{1,2} are extended, luminous, but rare structures that appear to be associated with the highest peaks in the matter density of the Universe³⁻⁶. Their energy output and morphology are similar to powerful radio galaxies⁷, but the source of the luminosity is unclear. Some blobs are associated with ultraviolet or infrared bright galaxies, suggesting an extreme starburst event or accretion onto a central black hole⁸⁻¹⁰. Another possibility is gas that is shock excited by supernovae^{11,12}. However some blobs are not associated with galaxies^{13,14}, and may instead be heated by gas falling into a dark matter halo¹⁵⁻¹⁹. The polarization of the Ly α emission can in principle distinguish between these options²⁰⁻²², but a previous attempt to detect this signature returned a null detection²³. Here we report on the detection of polarized Ly α from the blob LAB1². Although the central region shows no measurable polarization, the polarized fraction (P) increases to ≈ 20 per cent at a radius of 45 kpc, forming an almost complete polarized ring. The detection of polarized radiation is inconsistent with the in situ production of Ly α photons, and we conclude that they must have been produced in the galaxies hosted within the nebula, and re-scattered by neutral hydrogen.

The Ly α emission line of neutral hydrogen is a frequently used observational tracer of evolving galaxies in the high redshift Universe. Ly α imaging surveys typically find a large number of faint unresolved objects and a small fraction of extremely luminous and spatially extended systems that are usually referred to independently as Lyman alpha blobs (LABs). The compact sources usually appear to be more ordinary star forming galaxies whereas, since their discovery, much controversy has surrounded the true nature of LABs. Because one of the possible modes of powering LABs is the accretion of gas from the intergalactic medium¹⁵⁻¹⁹, an eventual consensus about this powering mechanism holds particular relevance for how the most massive and rapidly evolving high redshift dark matter haloes acquire the gas required to fuel star formation in the galaxies they host. Predictions for polarized Ly α radiation were made over a decade ago²⁰, and have been further developed to the extent that the polarization signal may act as a diagnostic to study the origin of the Ly α photons²¹. By relying upon the scattering of Ly α photons at large distances from their

production sites, these polarization measurements may also provide an independent constraint on the distribution of neutral gas in the circumgalactic regions, which has proven a difficult measurement to make by traditional techniques. The one previous attempt to detect the polarization of a LAB returned a null result²³, although very deep observations are required that need considerable time investments on 8–10 meter class telescopes. In the ESO Very Large Telescope observations presented here, we observe one of the largest and most luminous LABs on the sky in imaging polarimetry mode (Figs 1 and 2).

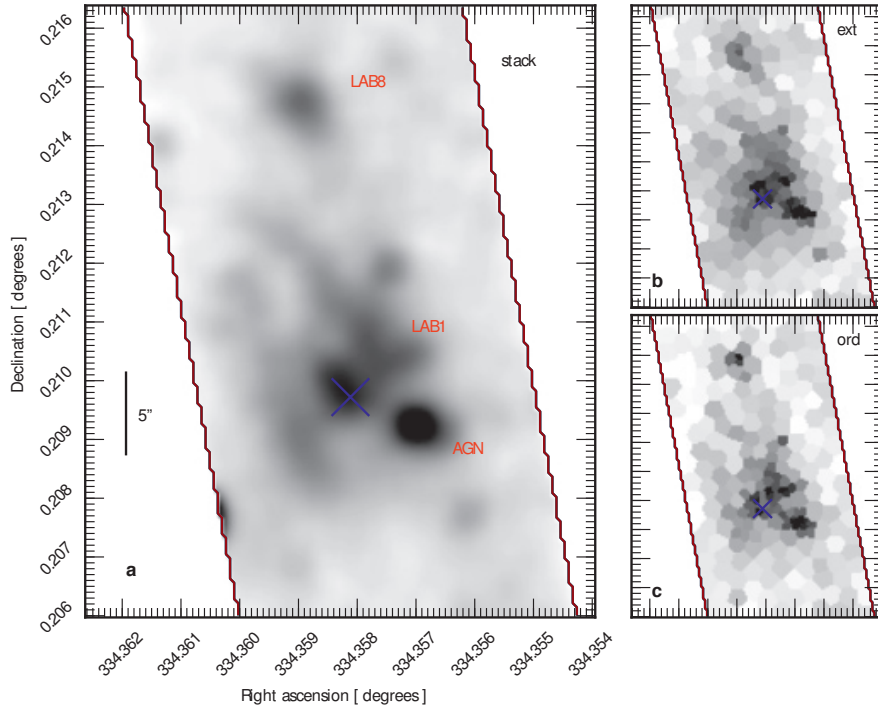


Figure 1 | LAB1 in Ly α . The large panel to the left shows the combined intensity frame that has been adaptively smoothed in order to show detail. The Ly α emission is spatially extended over scales of more than 10 arcsec (80 kpc). The 5 arcsecond scale bar shown in the left panel corresponds to 40 physical kilo-parsec. North is up and East is to the left. The primary target of this observation is LAB1², although the position angle was chosen so as to also include LAB8⁴, which resides some 20 arcsec to the North. The bright point source to the South East (lower right) is the AGN C11². Major centres are labelled in the image. The two smaller frames to the right show the ordinary and extraordinary beams (lower and upper, respectively), which have been tessellated for quantitative analysis (Supplementary Information). All images are shown on the same intensity scaling, and even by eye differences in the intensity structure between the two beams become visible. The cross marks the point that we determine to be the centre in the subsequent analysis, and is determined as the point of peak Ly α surface brightness that is not associated with the AGN.

These new, deep polarimetric observations show a substantial fraction of the Ly α emission

from LAB1 to be polarized. The data enable the fraction of light that is linearly polarized (P) to be measured to better than 5% (r.m.s.) in the regions of peak surface brightness, however in these central regions we find essentially no polarization signal. In order to detect the polarized emission we need to examine the fainter signal emanating a few arcsec from the centre – when Ly α is emitted with a high polarization fraction ($P \approx 20\%$), it is not spatially coincident with the brighter regions of the nebula. Indeed the highest and most statistically certain measures of P are found some 4–8 arcsec from the centre, forming an almost complete ring of polarized emission. Just a single resolution element shows a signal-to-noise ratio on P that exceeds 3, but our confidence in these results is substantially enhanced by the strong degree of spatial correlation between the resolution elements that are observed to be polarized at high significance. Away from the regions of bright Ly α emission our data show no measurable polarization signal, but a second nearby extended Ly α source (LAB8⁴) that lies to the north also shows strongly polarized Ly α .

Ly α is a resonant line and photons scatter in neutral hydrogen (H I), undergoing a complicated radiation transfer. At each scattering event, of which there may be millions, a photon acquires a new direction and frequency, dependent upon the kinematics of the scattering medium and quantum mechanical probabilities²⁴. The outgoing frequency determines the optical depth that the photon then sees^{25,26}: small shifts from line-centre (core scatterings) result in effectively no transfer, while long frequency excursions (wing scatterings) result in significant flights and likely escape from the system. The more frequent core scatterings may emit polarized radiation but it is typically with a low fraction ($P \lesssim 7\%$); the comparatively rare wing scatterings, on the other hand, may introduce a high degree of linear polarization to the outgoing radiation (P up to 40%)^{21,24}. The observed polarization signal therefore provides an unambiguous signature of the scattering nature of the diffuse Ly α halos, and distribution of circumgalactic gas. On the atomic level, the detected polarization signal provides evidence that the Ly α photons are not emerging after a large number of resonant core scattering events, but are exiting after long shifts in frequency.

The detection of polarization demonstrates that the Ly α photons cannot have been produced in situ at large radial distances. In order to impart a significant level of polarization on the outgoing radiation, a geometry is required in which Ly α photons preferentially escape after scattering off hydrogen atoms at angles of 90 degrees to their vector prior to the scattering event^{21,24}. This geometry is not expected in the case of wind/shock excitation since thermalized cooling gas will generate Ly α photons with no preferential orientation or impact angle with respect to the scattering medium. Similarly, the filamentary streams of cold infalling gas predicted by simulation^{27,28} appear to have too small volume filling factors, and be too narrow (few kpc) for any imparted polarization signal to be observable¹⁷ – a spatial resolution would be required that is currently unattainable by optical polarimeters. While neither of these rejected scenarios have yet been thoroughly tested by radiative transport studies, the production of polarized Ly α is well understood, and it is difficult to see a mechanism by which observably polarized Ly α may be produced in these situations. We therefore conclude that the Ly α photons must have been produced centrally in the galaxies themselves and scattered at large radii by neutral gas. Even if the halo is accreting intergalactic gas, this process is not responsible for a large fraction of the Ly α emission.

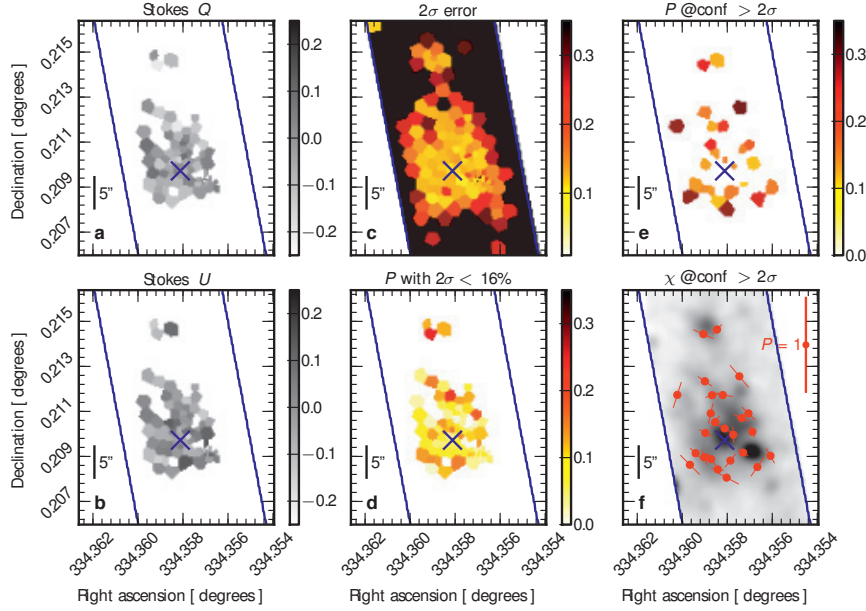


Figure 2 | The polarization of LAB1. Scaling is shown to the right of each panel. Panels (a) and (b) show the Q and U Stokes parameters. Panel (c) shows a map of the polarization fraction P that we can measure at 95.4% confidence; this error map demonstrates that in individual resolution elements we can constrain P in the central regions down to 10% (2σ). At a radius of $\approx 6 - 7$ arcsec, this decreases to about the 20% level, and beyond ≈ 10 arcsec P becomes noise-dominated. Panel (d) shows the value of P in resolution elements where it can be well constrained; we make a cut based on the error map, and show bins where P can be measured to better than 16% (2σ). P of around 5–10% is found in the centre, but increases to 15–20% at ≈ 5 arcsec from the centre towards the South, West, and North edges of LAB1. $P \approx 20\%$ is also seen around LAB8. Panel (e) shows P in bins for which we can be at least 95.4% confident of its measurement. The structure around LAB1 and LAB8 remains, extending to larger radii, and forming a broken ring at $P \sim 20\%$. Panel (f) shows a smoothed intensity image with the direction of the polarization vector, χ , shown by red bars. As with panel (e) only bins showing measurements at more than 95.4% confidence level are shown. There is a clear trend that, when bins show strong polarization, they orientate themselves tangentially to the overall structure and local Ly α surface brightness. These features conform well with the predictions for the polarization of Ly α photons that are centrally produced and scatter at large radii, or are produced by cooling gas that flows onto the dark matter halo in quasi spherical symmetry²¹.

The geometrical origin of the polarization signal in the photon scattering model, which is analogous to Rayleigh scattering, implies also that the angle of the polarization vector χ should align tangentially to the overall geometry of the system at large radii^{21,22}. We also extract this χ vector from the data (Fig 2, panel f). If we define the geometric centre to be the region of peak Ly α surface brightness (excluding the active nucleus; Fig 1), these vectors display a strong tendency to

orientate along directions tangential to the overall geometry of the system. Again this is in good agreement with theoretical expectations, should the Ly α photons be produced centrally by ordinary star-formation and/or AGN-fueled processes and scatter at large radii²¹. However unlike the idealized models used for radiative transport simulations, which assume perfect spherical symmetry and no velocity shear or clumping of the gas, the true Ly α surface brightness is far from smooth and symmetric. This may reflect either multiple Ly α sources within the halo, large scale inhomogeneities in the scattering medium, or both. Polarization of Ly α emission in a clumpy medium has not yet been tested by simulation although clumping could potentially either suppress or enhance the polarization²¹, and likely depends on the relative size and volume filling factor of the clumps. Regardless, we would still expect the polarization signature to remain provided that the individual regions are well resolved, in which case χ would then be expected to align tangentially to contours in the local surface brightness. This effect is also reflected in the data, and we find polarization vectors preferentially line up at angles approximately perpendicular to the local surface brightness gradient at their position. The Supplementary Information includes a quantitative analysis of the polarization angles compared with both local surface brightness gradients and the overall system geometry.

There is one final observable prediction that has been suggested by radiative transport simulations. This is the radial profile of the polarization fraction, P , which according to the scattering shell model should present with $P \approx 0$ in the geometric centre and increase with increasing radius. We have computed this radial profile of P using the same central coordinates as defined previously (Fig 3) and find strong evidence for P increasing with radius, again in agreement with predictions. The central point on the profile and most significantly polarized point in the ring are discrepant at over 2σ . We have fitted the innermost 7 arcsec (5 data points; where data are deemed reliable) with the simplest function for P varying linearly with radius. Computing the classical p -value, $1 - \Gamma(\nu/2, \chi^2/2)$ where ν is the number of degrees of freedom, shows above 96% confidence in this hypothesis. The same test performed on a flat profile ($P = 8.3\%$), suggests that a structure in which P is independent of radius is consistent with the data at 16%. Regardless, the slim possibility of P that is flat with radius does not present a difficulty for the scattering scenario, which is supported not only by the detection of polarized Ly α itself, but also by the angular distribution of polarization vectors; this radial profile is simply the least robust of our constraints. The actual gradient of P with radius depends upon both the column density and radius of the shell, neither of which we know – assuming that the idealized geometry holds and that the shell has a radius of 10 arcsec, the models with column densities of $10^{19} - 10^{20} \text{ cm}^{-2}$ would be in agreement with the data (Fig 3). In this step of the analysis we also compute the total luminosity-weighted polarization fraction within each radius: within 7 arcsec we obtain an integrated value of $P = 11.9 \pm 2\%$. We take this value as the overall polarization fraction of the nebula, which we quote at 6σ significance.

1. Francis, P. J. *et al.* A Group of Galaxies at Redshift 2.38. *Astrophys J.* **457**, 490–499 (1996). [arXiv:astro-ph/9511040](https://arxiv.org/abs/astro-ph/9511040).
2. Steidel, C. C. *et al.* Ly α Imaging of a Proto-Cluster Region at $\langle z \rangle = 3.09$. *Astrophys J.* **532**,

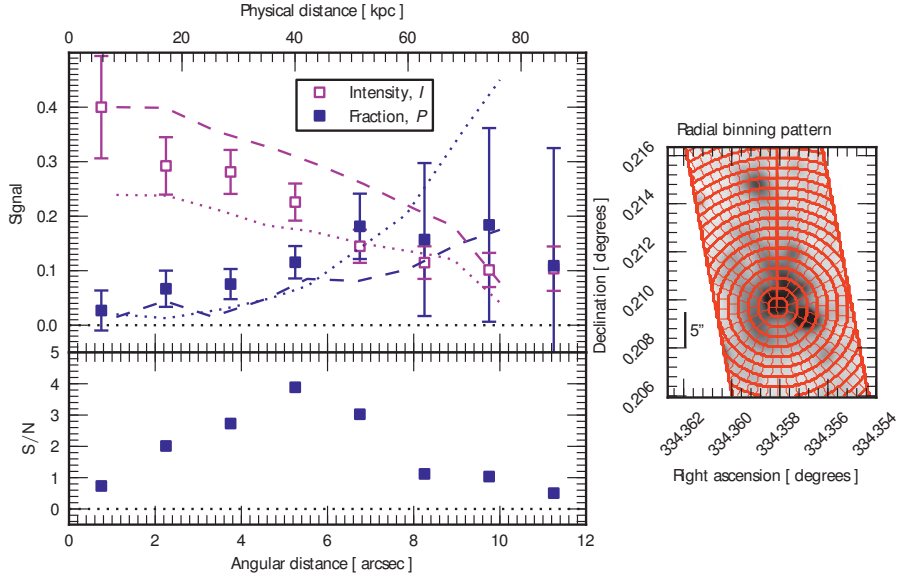


Figure 3 | The radial polarization profile. Blue points show the fractional polarization, P , which is measured in concentric 1.5 arcsec annuli. We implement a new binning method (Supplementary Information) that enables annular measurements of P using independent bins. The binning structure is shown to the right, the centre the same as illustrated in Fig 1. P has been corrected for spuriously high polarization fractions that may be measured at low signal-to-noise²⁹. In magenta the total intensity profile is shown. Errorbars on both measurements are 1σ , and the lower profile shows the signal-to-noise ratio of P . In the central regions where intensity is highest, P is measured at $\sim 4\%$, although at 1σ is consistent with no polarization. P and its signal-to-noise both increase with radius; by 5 arcsec $P = 10\%$ and is inconsistent with zero at the 4σ level. P peaks at 18% at 7 arcsec, beyond which radius the noise becomes dominant. Overlaid are the results of numerical models for scattered Ly α radiation²¹ in an expanding H I shell with two column densities: 10^{19} cm^{-2} (lower) and 10^{20} cm^{-2} (upper). The curves have been smoothed over lengths of 1.5 arcsec to match our annuli. The actual radius of the shell is unknown, so the theoretical points have been scaled to shell radius of 10 arcsec, in order to approximately match both the surface brightness and polarization profiles. This shows that the predictions are qualitatively matched by observation. Models for scattering in a static IGM and spherically symmetric accretion are not shown since they are not leading explanations for the powering of LABs.

- 170–182 (2000). arXiv:astro-ph/9910144.
3. Palunas, P., Teplitz, H. I., Francis, P. J., Williger, G. M. & Woodgate, B. E. The Distribution of Ly α -Emitting Galaxies at $z=2.38$. *Astrophys J.* **602**, 545–554 (2004). arXiv:astro-ph/0311279.
 4. Matsuda, Y. *et al.* A Subaru Search for Ly α Blobs in and around the Protocluster Region At Redshift $z = 3.1$. *Astron. J.* **128**, 569–584 (2004). arXiv:astro-ph/0405221.
 5. Yang, Y., Zabludoff, A., Tremonti, C., Eisenstein, D. & Davé, R. Extended Ly α Nebulae at z sime 2.3: An Extremely Rare and Strongly Clustered Population? *Astrophys J.* **693**, 1579–1587 (2009). 0811.3446.
 6. Prescott, M. K. M., Kashikawa, N., Dey, A. & Matsuda, Y. The Overdense Environment of a Large Ly α Nebula at $z \sim 2.7$. *Astrophys J. Lett.* **678**, L77–L80 (2008). 0803.4230.
 7. Saito, T. *et al.* Systematic Survey of Extended Ly α Sources over $z \sim 3-5$. *Astrophys J.* **648**, 54–66 (2006). arXiv:astro-ph/0605360.
 8. Geach, J. E. *et al.* The Chandra Deep Protocluster Survey: Ly α Blobs are Powered by Heating, Not Cooling. *Astrophys J.* **700**, 1–9 (2009). 0904.0452.
 9. Scarlata, C. *et al.* He II Emission in Ly α Nebulae: Active Galactic Nucleus or Cooling Radiation? *Astrophys J.* **706**, 1241–1252 (2009).
 10. Colbert, J. W. *et al.* Polycyclic Aromatic Hydrocarbon Emission within Ly α Blobs. *Astrophys J.* **728**, 59–71 (2011).
 11. Taniguchi, Y. & Shioya, Y. Superwind Model of Extended Ly α Emitters at High Redshift. *Astrophys J. Lett.* **532**, L13–L16 (2000). arXiv:astro-ph/0001522.
 12. Mori, M., Umemura, M. & Ferrara, A. The Nature of Ly α Blobs: Supernova-dominated Primordial Galaxies. *Astrophys J. Lett.* **613**, L97–L100 (2004). arXiv:astro-ph/0408410.
 13. Nilsson, K. K., Fynbo, J. P. U., Møller, P., Sommer-Larsen, J. & Ledoux, C. A Lyman- α blob in the GOODS South field: evidence for cold accretion onto a dark matter halo. *Astron. Astrophys.* **452**, L23–L26 (2006). arXiv:astro-ph/0512396.
 14. Smith, D. J. B. & Jarvis, M. J. Evidence for cold accretion onto a massive galaxy at high redshift? *Mon. Not. R. Astron. Soc.* **378**, L49–L53 (2007). arXiv:astro-ph/0703522.
 15. Fardal, M. A. *et al.* Cooling Radiation and the Ly α Luminosity of Forming Galaxies. *Astrophys J.* **562**, 605–617 (2001). arXiv:astro-ph/0007205.
 16. Yang, Y. *et al.* Probing Galaxy Formation with He II Cooling Lines. *Astrophys J.* **640**, 539–552 (2006). arXiv:astro-ph/0509007.

17. Dijkstra, M. & Loeb, A. Ly α blobs as an observational signature of cold accretion streams into galaxies. *Mon. Not. R. Astron. Soc.* **400**, 1109–1120 (2009). 0902.2999.
18. Goerdt, T. *et al.* Gravity-driven Ly α blobs from cold streams into galaxies. *Mon. Not. R. Astron. Soc.* **407**, 613–631 (2010). 0911.5566.
19. Faucher-Giguère, C.-A., Kereš, D., Dijkstra, M., Hernquist, L. & Zaldarriaga, M. Ly α Cooling Emission from Galaxy Formation. *Astrophys J.* **725**, 633–657 (2010). 1005.3041.
20. Lee, H. & Ahn, S. Polarization of the Ly alpha from an Anisotropy Expanding H I Shell in Primeval Galaxies. *Astrophys J. Lett.* **504**, L61–L64 (1998). arXiv:astro-ph/9803085.
21. Dijkstra, M. & Loeb, A. The polarization of scattered Ly α radiation around high-redshift galaxies. *Mon. Not. R. Astron. Soc.* **386**, 492–504 (2008). 0711.2312.
22. Rybicki, G. B. & Loeb, A. Polarization of the LYalpha Halos around Sources before Cosmological Reionization. *Astrophys J. Lett.* **520**, L79–L81 (1999). arXiv:astro-ph/9903291.
23. Prescott, M. K. M., Smith, P. S., Schmidt, G. D. & Dey, A. The Line Polarization within a Giant Ly α Nebula. *Astrophys J. Lett.* **730**, L25–L30 (2011). 1102.3918.
24. Stenflo, J. O. Resonance-line polarization. V - Quantum-mechanical interference between states of different total angular momentum. *Astron. Astrophys.* **84**, 68–74 (1980).
25. Adams, T. F. The Escape of Resonance-Line Radiation from Extremely Opaque Media. *Astrophys J.* **174**, 439–448 (1972).
26. Neufeld, D. A. The transfer of resonance-line radiation in static astrophysical media. *Astrophys J.* **350**, 216–241 (1990).
27. Kereš, D., Katz, N., Weinberg, D. H. & Davé, R. How do galaxies get their gas? *Mon. Not. R. Astron. Soc.* **363**, 2–28 (2005). arXiv:astro-ph/0407095.
28. Dekel, A. & Birnboim, Y. Gravitational quenching in massive galaxies and clusters by clumpy accretion. *Mon. Not. R. Astron. Soc.* **383**, 119–138 (2008). 0707.1214.
29. Wardle, J. F. C. & Kronberg, P. P. The linear polarization of quasi-stellar radio sources at 3.71 and 11.1 centimeters. *Astrophys J.* **194**, 249–255 (1974).

Acknowledgements Based on observations made with ESO Telescopes at the Paranal Observatory under programme ID 084.A-0954. M.H. was supported in part by the Swiss National Science Foundation, and also received support from Agence Nationale de la recherche bearing the reference ANR-09-BLAN-0234-01. Patrick Ogle is thanked for his valuable suggestions about polarimetric observations. We are indebted to Nino Panagia and Terry Jones for comments on the manuscript, and to Daniel Schaerer, Nick Scoville, Chris Lidman, Arjun Dey, Moire Prescott, and Paul Lynam for discussions.

Author Contributions All authors contributed to the proposal preparation. M.H. and C.S. observed and reduced the data. M.H. analyzed the results. All authors contributed to the manuscript preparation.

Competing Interests The authors declare that they have no competing financial interests.

Correspondence Correspondence and requests for materials should be addressed to M.H. (email: matthew.hayes@ast.obs-mip.fr).